Explaining the hydrological behaviour of facultative phreatophytes using a multi-variable and multi-objective modelling approach

Cristina Puertes[1], Antonio Lidón[1], Carlos Echeverría[1], Inmaculada Bautista[1], María González-Sanchis[1], Antonio D. del Campo[1], Félix Francés[1]

[1]Research Institute of Water and Environmental Engineering (IIAMA), Universitat Politècnica de València, Camino de Vera s/n, E-46022 Valencia, Spain

Corresponding author: Cristina Puertes (cripueca@cam.upv.es)

Abstract

Trees in semi-arid conditions survive despite water scarcity and shallow soils because they commonly have access to subsoil water resources. Currently, conventional models do not include groundwater transpiration and the results frequently underestimate the actual evapotranspiration and overestimate the net recharge. Therefore, in this work we focus on how a multi-variable calibration with a multi-objective approach may improve model robustness leading to a more realistic closure of the water balance in two models (LEACHM and TETIS) of different conceptualisation taking into account the specific characteristics of a facultative phreatophytic forest. The results suggest that the common single-variable and single-objective calibration is not able to measure all system's characteristics. However, the multi-variable and multi-objective calibration proved a good option to reproduce the water dynamics of a facultative phreatophytic forest and confirmed that groundwater transpiration is an important water source for them. Therefore, hydrological models should include this mechanism and both LEACHM and TETIS proved an acceptable tool to be applied in the regions covered by these species.

1 Introduction

Semiarid areas are characterised by their limited water availability, shallow soils (Eliades et al., 2018) and deep groundwater table (Fan et al., 2013). Trees in water-limited environments are exposed to long dry seasons and many species have developed several adaptation mechanisms (Lubczynski, 2009; Rodriguez-Iturbe et al., 2001). One of these mechanisms is the development of deep groundwater tapping roots. These species are termed facultative phreatophytes, characterised by the infrequent or partial use of groundwater resources to survive (Macfarlane et al., 2018), a process commonly known as “groundwater transpiration”. *Quercus ilex* (holm oak) is one of the main Mediterranean evergreen oaks in the Iberian Peninsula that grows in its semiarid areas. In these environments, *Q.ilex* has developed the morphological adaptive mechanism of deep tap roots (Barbeta and Peñuelas, 2016) and its rooting system can reach depths up to 3.7 m (Canadell et al., 1996). Therefore, *Q.ilex* is able to access the water table or extend its root system through fractured rock to access stored water (Schwinning, 2010).

Most of these *Q. ilex* forests grow in the upper part of catchments and their actual evapotranspiration can heavily influence downstream water availability (Vicente et al., 2018). Globally, mean annual evapotranspiration accounts for 67% of mean annual precipitation (Zhang et al., 2016), while this value can exceed 85% (Morillas et al., 2013; Piñol et al., 1991; Yaseef et al., 2010) in water-limited environments, such as complex Mediterranean ecosystems with wide inter- and intra-annual precipitation variability (Gallart et al., 2002; García-Ruiz et al., 2011). Thus groundwater transpiration in these ecosystems cannot be neglected, and several studies have shown its key contribution to total plant transpiration (Barbeta and Peñuelas, 2017; David et al., 2004; Miller et al., 2010; Swaffer et al., 2014; Witty et al., 2003). Nevertheless, this groundwater transpiration is not often considered when conventional hydrological models are used and, consequently, the results frequently underestimate the actual evapotranspiration and overestimate the net recharge (Balugani et al., 2017; Eliades et al., 2018).

Hence, more attention needs to be paid to groundwater transpiration because it is a critical aspect, and one that should be included in the hydrological models used under semiarid conditions to obtain a more realistic water balance closure. For this reason, and in order to not make the conclusions model-dependent, two models with different conceptualisations were calibrated in this study using the experimental data recorded in a *Q. ilex* experimental plot with a semiarid climate. Soil moisture, interception and transpiration measurements are available, and the impairment between soil moisture and transpiration during summer drought periods suggests that *Q. ilex* may have access to subsoil water resources, at least during these periods (del Campo et al., 2019a; Vicente et al., 2018).

The first model was the widely used LEACHM model (Hutson, 2003). LEACHM is a process-based model that was developed to simulate water and solute transport in unsaturated or partially saturated soils. The second model was based on the parsimonious conceptual eco-hydrological model TETIS (Pasquato et al., 2015; Ruiz-Pérez et al., 2016a), which was adapted to incorporate groundwater transpiration.

Both LEACHM and TETIS models are, however, mathematical representations of reality in a simplified form. Their parameters are representative of the modelling scale and differ from those measured in the field (Mertens et al., 2005). Therefore, model calibration is crucial but, generally, a single criterion in a calibration process does not suffice to measure all system's characteristics (Guo et al., 2013; Yapo et al., 1998). Single-variable and single-objective calibration may lead to a hydrologically parameter set not being considered acceptable (Vrugt et al., 2003) because the potential for obtaining equally acceptable fits to observational data with different parameter sets increases. This problem, introduced by Beven (1993), is called equifinality, and these non-hydrologically acceptable parameter sets are called non-behavioural. Hence in order to reduce them by constraining the model, many studies have used multi-site (Cao et al., 2006; Hasan and Pradhanang, 2017; Her and Chaubey, 2015; Nkiaka et al., 2018; Zhang et al., 2015) and multi-variable (Haas et al., 2016; López López et al., 2016; Medici et al., 2012; Rientjes et al., 2013) calibrations.

Three different calibration approaches were considered herein: (1) single-variable and single-objective calibration by using soil water content as the target; (2) single-variable and single-objective calibration by using transpiration as the target; (3) multi-variable and multi-objective calibration by using both soil water content and transpiration and, additionally, interception only in the case of TETIS (LEACHM does not consider interception). These results were compared to one another and the results obtained with the multi-variable and multi-objective approach were analysed in-depth.

Within this framework, this study firstly aims to better understand the hydrological behaviour of facultative phreatophytes with two models of different conceptualisations, and by means of a multi-variable and multi-objective calibration. It secondly aims to serve as a springboard to improve future hydrological models to make them more suitable to be applied in regions covered by such species. And finally, as the Mediterranean region has shown a negative precipitation trend throughout the 20th century (Cook et al., 2018), and as it stands out in climate change projections as an area where total drought severity increases in either scenario (Spinoni et al., 2018), it aims to improve future predictions.

2 Materials and Methods

2.1 Study area

The study area (Fig.1) is an experimental plot covering 1,800 m^2 located in the forest *Monte de la Hunde* in east Spain (39°04’29-30’’ N, 1°14’25-26’’ W elevation 1,080-1,100 m a.s.l.). It corresponds to the non-treated plot described in del Campo et al. (2019a). Soil texture is loam with a high degree of stoniness, a basic pH and high calcium carbonate content (Table 1). The slope is 31% with a NW aspect. Soil thickness ranges from 10 cm to 40 cm, and underneath a karstified Jurassic limestone parent rock arises with faults and fissures, which were revealed by the boreholes (depth up to 4 m) drilled all over the plot (del Campo et al., 2019b). The water table was not found within these 4 m, but the parent rock is a significant reservoir of deep water (del Campo et al., 2019b). The mean annual precipitation, temperature and reference evapotranspiration (Hargreaves and Samani, 1985), are respectively 466 mm, 12.8°C and 1,200 mm, according to the meteorological dataset (1960-2011) of a nearby weather station. According to the Köppen climate classification, it is a water-limited environment with a semiarid climate. The forest is a high-density stand of *Q. ilex* where other species (*Pinus halepensis, Q. faginea, Juniperus phoenicea and J. oxycedrus*) are barely present. The forest structure was characterised in May 2012 and the results were: 10.7 cm and 7.7 cm of diameter at the basal and breast heights, respectively, 5.6 m^2 ha^{-1} basal area and a density of 1,059/1,133 trees ha^{-1} (holm oak/all trees) (del Campo et al., 2019a). The Leaf Area Index (LAI) was seasonally measured (approximately 3 times a year) and the average measured value was 1.13±0.22 m^2 m^{-2} (2012-2016).

Layer	Stoniness (%)	pH	$CaCO_3$ (%)	SOC (g kg^{-1})	Texture
L Layer	48.4±10.7				
H Layer	59.2±7.1	7.84±0.09	15.3±5.6	131.2±32.0	
0-10 cm	63.9±8.5	8.05±0.11	21.1±6.7	73.2±17.4	44; 33; 23
10-30 cm	58.6±7.3	8.25±0.12	34.1±6.2	42.3±21.4	57;23;20
30-40 cm	55.5±7.2	8.34±0.04	36.7±1.7	25.1±6.4	48;32;19

Table 1 Soil characteristics of the study site. SOC means soil organic carbon. Particle fractions in the following order: sand, silt and clay (%).(Bautista et al., 2015; del Campo et al., 2018)

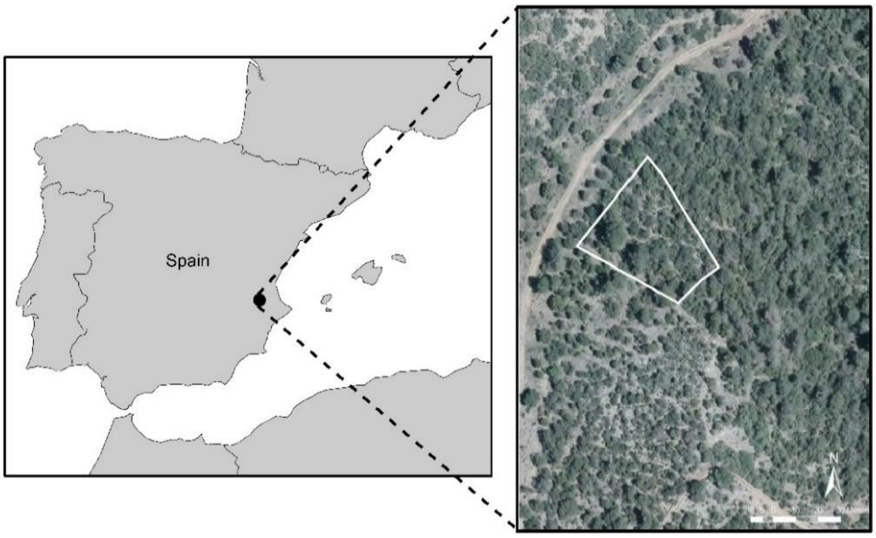

Figure 1 Location of the experimental plot study site

2.2 Meteorological data and field measurements

In this plot, all the meteorological data and field measurements were recorded every 10 minutes, and averaged on a daily basis during the observational period from 01/10/2012 to 26/04/2016.

Air temperature and relative humidity were recorded by a Decagon Device T/RH sensor at a 2-metre height above the ground surface. Precipitation was continuously measured in an open area 20 m away from the plot using a Davis tipping bucket rain gauge with a resolution of 0.2 mm. Throughfall was measured according to the methodology described in del Campo et al. (2018).

The soil water content measurements were taken with a Decagon Device EC-5. Fifteen probes were installed at depths of 5, 15, and 30 cm. The default calibration of the probes for the mineral soils was used. Runoff was measured in a collecting trench by a Diehl Metering Altair v4 volumetric counter.

The heat ratio method (Burgess et al., 2001) was followed to measure sap flow velocity in 14 trees, which were divided into four different diametrical distributions. In each tree, an ICT International sap flow sensor was installed on the north trunk side. These measurements were upscaled to stand transpiration, and accounted for tree density and tree diameter frequency distribution.

It should be highlighted that in summer months, a positive difference between transpiration and soil water content changes was observed (i.e. transpiration > soil water content changes) (Fig. 2). This impairment between soil moisture and transpiration during summer drought periods is only possible if *Q.ilex* takes groundwater resources, hence the hypothesis of additional groundwater transpiration is justified.

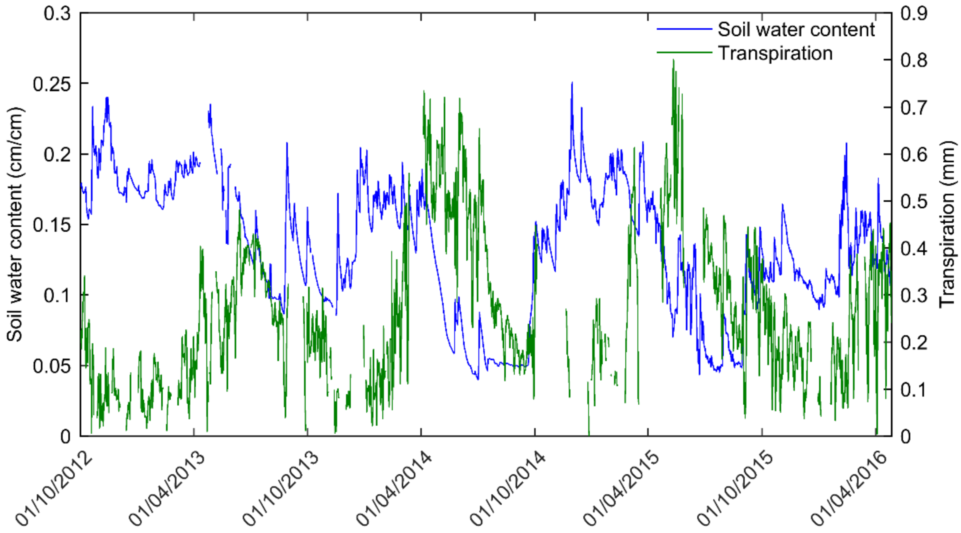

Figure 2 Observed soil water content and transpiration series

The LAI was seasonally measured in the field 12 times during the observational period by an LAI-2000 sensor. The series was completed with estimations made from the level-4 MODIS global LAI satellite product (NASA, LPDAAC). The MODIS LAI dataset was reprojected on the UTM projection system, and linear regression was calculated between it and the LAI measured in the field to adjust the MODIS LAI dataset. The resultant LAI was linearly interpolated to obtain daily results.

A complete description of the methodology employed to obtain the meteorological variables and field measurements can be found in del Campo et al. (2018) and in del Campo et al. (2019a).

2.3 The LEACHM and TETIS models

On the one hand, this study used the LEACHM model (Hutson, 2003), which has been widely used for simulating water and solutes movement in unsaturated soils (Asada et al., 2013; Deng et al., 2017; Lidón et al., 2013; Nasri et al., 2015). LEACHM is a one-dimensional model that divides the soil profile into a user's fixed number of horizontal layers of equal thickness. It employs finite differencing approximation and is composed of 24 parameters. Nine of these parameters are defined for each soil layer and, therefore, using more layers considerably increases the number of parameters to be estimated or calibrated.

On the other hand, the TETIS eco-hydrological model (GIMHA, 2018) was also used. It is a conceptual model based on a tank type conceptualisation (Fig. 3) and water moves downwardly as long as the tank outflow capacity is not exceeded. TETIS divides soil into two horizontal layers, and is composed of 20 parameters and one correction factor used to adjust total evapotranspiration. Additionally, the model offers the possibility of activating a dynamic vegetation submodel. However, for simplicity, the LAI values simulated by the dynamic vegetation submodel were introduced as inputs, keeping the vegetation submodel deactivated.

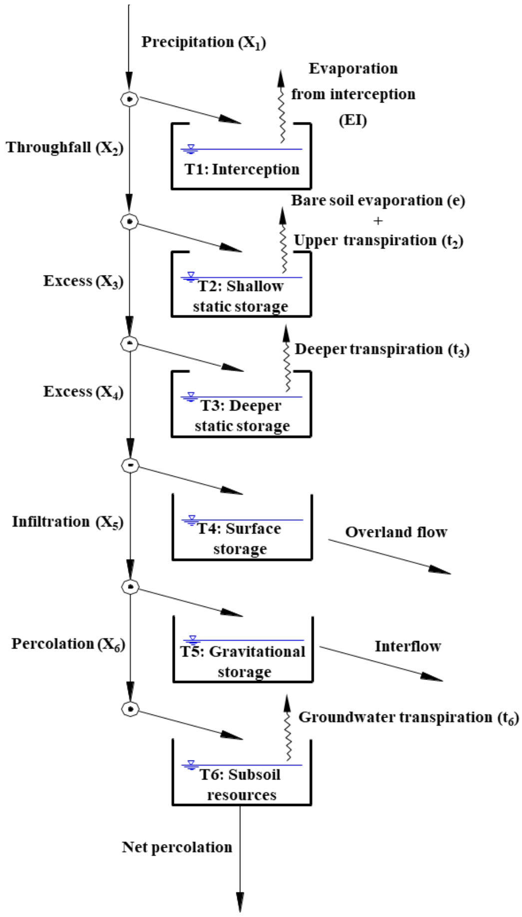

Figure 3 Schema of the adapted TETIS hydrological submodel to the case study

The main difference between both models is the way in which water flow in the unsaturated zone is calculated. LEACHM employs Richards' equation and is solved by the Crank and Nicolson (1947) implicit method:

$$\frac{\partial\theta}{\partial t}=\frac{\partial}{\partial z}\left[K(\theta)\frac{\partial h}{\partial z}+1\right]-U(z,t) \qquad (1)$$

where θ is volumetric water content (m^3 m^{-3}), h is soil water pressure head (mm), $K(\theta)$ is hydraulic conductivity (mm day^{-1}) at the θ water content, t is time (day), z is depth (mm) and $U(z,t)$ is plant transpiration, represented as water lost per unit time (day^{-1}). Although some calculations are made daily, this equation is solved for each soil layer and each water flow interval, with a periodicity of 0.1 day, or less, and may be automatically reduced during high water flux periods. The model offers the possibility of simulating a fixed depth water table as the lower boundary condition. The hydraulic head gradient is assumed to be zero between the phreatic surface and the bottom of the simulated profile and, hence, upward water flow is considered (capillary fringe). Thus no modification in the code is needed to reproduce the facultative phreatophytes' behaviour. The soil water pressure head and hydraulic conductivity are calculated as proposed by Campbell (1974):

$$h=a(\theta/\theta_s)^{-b} \qquad (2)$$

$$K(\theta)=K_s\,(\theta/\theta_s)^{2b+2+p} \qquad (3)$$

where K_s is hydraulic conductivity at saturation (mm day^{-1}), θ_s is volumetric water content at saturation (m^3 m^{-3}), a and b are constants, although a is sometimes regarded as an air-entry value, and p is a pore interaction parameter set at 1 in the code. If infiltration capacity is exceeded, the difference is assigned to runoff. The water infiltration depth is reduced according to both the SCS curve number approach and the slope (Williams, 1991).

In contrast, TETIS employs simpler equations. The first tank (T_1) represents the intercepted water, which can only exit by direct evaporation:

$$D_1(t) = min[X_1(t)\,;\; l_s\, LAI(t)\, f_c - T_1(t-1)] \tag{4}$$

where t is time, D_1 is the intercepted water (mm), X_1 is precipitation (mm), l_s is maximum leaf storage (mm), LAI is Leaf Area Index ($m^2\ m^{-2}$), f_c is vegetation cover factor and T_1 is the interception tank storage (mm). Tanks T_2 and T_3 represent the static storage of soil. Water flows to these tanks according to:

$$D_i(t) = min\left[X_i(t)\left(1 - \frac{T_i(t-1)}{Hu_i}\right)^{exp_i} ; Hu_i - T_i(t-1)\right] \tag{5}$$

where i refers to either the shallow soil layer (2) or the deeper soil layer (3), D_i is the water retained in soil by capillary action (mm), X_i is throughfall or excess (mm), T_i is the shallow or deeper static storage (mm), Hu_i is the maximum static storage water content of each layer (mm) and exp_i is a constant. This exponent takes values between 0 and 3. A value that differs from 0 means that there is excess before the static storage tank reaches its maximum capacity. Vertical flows are calculated as a balance in nodes. Hence any water not retained moves downwardly whenever the outflow capacity is not exceeded (surface infiltration capacity or percolation capacity). The excess supplies tanks T_4 and T_5, which act as linear storages characterised by residence times.

The other difference between both models is the way in which evapotranspiration is calculated. To simulate soil evaporation, LEACHM adjusts the soil water pressure head by changing the upper boundary condition of Richards' equation, and transpiration is calculated following Nimah and Hanks (1973):

$$U(z,t) = K(\theta,t)\,\frac{[H_{root} + z\,(R_c+1) - h(t) - s(t)]}{\Delta x \Delta z} RDF \tag{6}$$

where H_{root} is the water potential at the root-soil interface (mm), (R_c+1) is a root resistance term (mm), s is the osmotic potential (mm), RDF is the fraction of active roots in the soil layer, Δz is the soil layer thickness (mm) and Δx is the conceptual distance from the point where h and s are calculated to the plant root (fixed at 10 mm in the code). Daily potential evapotranspiration is calculated as one seventh of the weekly reference evapotranspiration values supplied by the user. It is split into potential evaporation and potential transpiration according to the vegetation cover fraction. Actual evaporation is calculated in accordance with the potential evaporation and the maximum possible evaporative flux density. The potential transpiration may be increased by the deficit if the actual evaporation is less than the potential evaporation.

TETIS calculates evaporation from the interception as:

$$EI(t) = min[ET_0(t)\, f_{ET}\ ;\ T_1(t)] \tag{7}$$

where EI is evaporation from the interception (mm), ET_0 is the potential evapotranspiration (mm) and f_{ET} is a correction factor for the total evapotranspiration. Therefore, transpiration is calculated using the remaining ET_0. This point is where TETIS has been improved. Firstly, the previous transpiration equation expressed the dependence of transpiration on the LAI as $min(1, LAI(t))$. This term indicates that transpiration is not reduced if the LAI is above 1. However, some studies have found that this LAI value is around 6 and varies depending on climate and vegetation (Granier et al., 2000; Li et al., 2019). Nevertheless, instead of fixing this value at 6, it was added as a parameter to be calibrated. It was called LAI_0 and represents the LAI value above which transpiration is not limited because of the LAI. Secondly, the possibility of transpiration from an intermediate tank (T_6) between the soil and the aquifer was added for this case study. Consequently, two new parameters were included: a soil moisture threshold ϑ_{GT} (cm cm^{-1}) and a groundwater root percentage Z_{gt}. The former represents the profile soil moisture value below which the groundwater resources transpiration is triggered. The groundwater root percentage represents the percentage of roots located in the second soil layer that grows through the fractured rock to access these subsoil water resources. The new equations used to calculate transpiration are:

$$t_2(t) = min\left[\left(ET_0(t)f_{ET} - EI(t)\right)\frac{min(LAI(t), LAI_0)}{LAI_0}\ \xi(t)Z_1\ f_c\ ;\ T_2(t)\right] \quad (8)$$

$$t_3(t) = min\left[\begin{pmatrix} \left(ET_0(t)f_{ET} - EI(t)\right)\frac{min(LAI(t), LAI_0)}{LAI_0}\ \xi(t)(Z_2\ + Z_{gt})\ f_c & \vartheta(t) \geq \vartheta_{GT} \\ \left(ET_0(t)f_{ET} - EI(t)\right)\frac{min(LAI(t), LAI_0)}{LAI_0}\ \xi(t)\ Z_2\ \ f_c & \vartheta(t) < \vartheta_{GT} \end{pmatrix};\ T_3(t)\right] \quad (9)$$

$$t_6(t) = min\left[\begin{pmatrix} 0 & \vartheta(t) \geq \vartheta_{GT} \\ \left(ET_0(t)f_{ET} - EI(t)\right)\frac{min(LAI(t), LAI_0)}{LAI_0}\ Z_{gt}\ f_c & \vartheta(t) < \vartheta_{GT} \end{pmatrix};\ T_6(t)\right] \quad (10)$$

where t_i is transpiration from soil layer i (mm), ξ is a water stress factor, *fc* is the vegetation cover factor and Z_i is the percentage of roots in layer i. The sum of Z_1, Z_2 and Z_{gt} should equal one. Soil evaporation is calculated as:

$$e(t) = min\left[\left(ET_0(t) - EI(t)\right)\xi(t)(1 - f_c)\ ;\ T_2(t)\right] \quad (11)$$

where *e* is soil evaporation and ξ is a water stress factor or a soil water limitation for bare soil.

2.4 Parameterisation and implementation

Hydrological models represent reality in a simplified form. Their parameters are representative of the modelling scale, but differ from those measured in the field (Mertens et al., 2005). These parameters are usually known as effective parameters and the main purpose of a calibration process is to obtain them, which is a priority to make precise predictions. The objective of these effective parameters is to compensate for the error in the model structure, the spatial and temporal scale effects, and the error in the measured inputs and output variables (Abbaspour et al., 2007; Francés et al., 2007).

2.4.1 Parameterisation and manual calibration

The simulation period of both models included the period with available observations (01/10/2012 to 26/04/2016), and a previous warming-up period (01/08/2012 to 30/09/2012) during which only meteorological data were available. The objective of the warming-up period was to eliminate the effect of the initial condition. The first two hydrological years were selected to calibrate the models and the remaining period was used to validate them. LEACHM was used with a 0.05 day time-step, although the output data are expressed daily. TETIS was used directly with a daily time-step. Both were implemented by using the field measurements of soil water content and transpiration. The soil water content data were daily averaged, but transpiration was averaged on a weekly basis because, as mentioned in Section 2.3, LEACHM employs the weekly reference evapotranspiration and, although daily results are calculated, it is expected to simply match the weekly transpiration value. The interception data were used in the calibration of TETIS. LEACHM does not consider the process of interception, and throughfall (net precipitation) is the required input. Therefore, as the interception process in TETIS is represented in a very simplified form, the interception data were used as accumulated for the whole calibration period to improve the hydrological annual balance representation and to reduce the error.

With LEACHM, some of the required parameters were already measured in the field and were not included in the calibration process. The parameters to be calibrated were the three hydraulic parameters for each soil layer, the root distribution of the soil profile, the vegetation cover fraction, the pan factor that corrects the potential evapotranspiration series, and the water table depth. LEACHM is able to represent the capillary fringe because it can consider a fixed water table. However soil depth is 30 cm in this case, but *Q. ilex* roots are deeper because this species is able to extend its root system through fractured rock. Hence, extra layers had to be added as an artefact to reproduce transpiration from fractured rock (groundwater transpiration). Consequently, six layers (5 cm thick) represented soil (30 cm) and 16 extra layers of the same thickness were added to represent the *Q. ilex* groundwater resources transpiration. All the layers had to have the same thickness in LEACHM. This number of extra segments was determined in an initial manual calibration because, as each layer has different parameters, it can lead to a cumbersome programming procedure. The initial calibration values used were those found in the literature, calculated from the soil texture data, field observations and previous experience (Table 2). The soil physical properties of the first six layers representing soil were grouped as pairs, and homogenous physical properties were considered in the 16 extra segments. From the 7^{th} layer, the percentage of roots was proportionally lowered in depth, and only the percentage of roots in the 7^{th} soil layer was calibrated. Soil water content and water flows were calculated until the 6^{th} soil layer because these layers are those that represent soil. Groundwater transpiration was calculated from the 16 extra layers, which represented fractured rock. These final parameters are listed in Table 2.

The TETIS eco-hydrological model at plot scale is composed of 20 parameters and one correction factor used to adjust total evapotranspiration (Table 3). In this case study, interflow was not observed throughout the monitoring period and, consequently, the percolation capacity and residence time in the gravitational storage took a value of infinite, which meant that all the water was percolated. Thereafter, the initial calibration was also carried out manually using the values recommended in the literature and by taking field observations and previous experience into account (Table 3).

2.4.2 Automatic calibration: from single- to multiple-objective approaches

Both models were automatically calibrated after the manual calibration. The automatic calibration was performed using the Multiobjective Shuffled Complex Evolution Metropolis (MOSCEM) algorithm (Vrugt et al., 2003), which is based on the concept of Pareto-optimal solutions. The interaction among the objective functions during the calibration process leads to a set of solutions, called Pareto front. This Pareto front represents the trade-offs among the different objectives with the property of improving the representation of one objective, while deteriorating the other one (Medici et al., 2012; Ruiz-Pérez et al., 2016b; Vrugt et al., 2003).

Population size was set at 50,000 and the number of complexes came to 200. The goodness-of-fit index selected to measure the performance of the models was the Nash and Sutcliffe efficiency index (EI) for soil water content (EI_{SWC}) and transpiration (EI_{TR}). EI_{SWC} was calculated from the daily results, while EI_{TR} was calculated from the weekly averaged results. The volume error was used to measure the performance of TETIS in reproducing the accumulated interception (VE_{int}). The algorithm was programmed to minimise the objective function. Thus instead of using the EI indices directly in the calibration, (1-EI) was used.

Three different calibration approaches were considered: (1) single-variable and single-objective calibration by using soil water content (Best EI_{SWC}); (2) single-variable and single-objective calibration by using transpiration (Best EI_{TR}); (3) multi-variable and multi-objective calibration by using soil water content, transpiration and accumulated interception with TETIS (Multi-variable). The single-objective and single-variable solutions were chosen from the extremes of the Pareto front, which correspond to the parameter sets with the lowest (1-EI_{SWC}) and (1-EI_{TR}) values (i.e. univariate solutions). With the multi-objective and multi-variable calibration, a compromise solution from the Pareto front was chosen according to these criteria: minimum Euclidean distance calculated using (1-EI_{SWC}) and (1-EI_{TR}) and VE_{int} less than 40% only with TETIS. The VE_{int} criteria were chosen to reduce the interception error in TETIS. The Euclidean distance is a mathematical criterion that represents the distance between a point of the Pareto Front and the ideal point (Guo et al., 2014; Herman et al., 2018). The ideal point is the point of the Pareto Front that simultaneously minimizes both criteria, (0,0) in this case.

The performances of both models using the multi-variable and multi-objective compromise solution were compared to that obtained using the single-variable and single-objective solution (soil water content and transpiration). The hydrological annual balances, groundwater transpiration and the distribution between the water that flows out of the ecosystem ("blue water") and evapotranspiration ("green water"), the B/G rate, were analysed in the multi-variable and multi-objective approach.

3 Results

The scatterplots shown in Figures 4 and 5 present the 50,000 function evaluations made by the MOSCEM algorithm (Vrugt et al., 2003). A point represents each model evaluation and its components represent the trade-offs in the decision space. With LEACHM, seven parameter sets formed the Pareto front, while 113 formed the Pareto front in TETIS, which included a third objective function (VE_{int}). The more the objective functions, the more the Pareto optimal solutions because the possible solution space enlarges (Khu and Madsen, 2005). The parameter values obtained during the calibration process for each calibration approach, chosen according to the above-described criteria, are compiled in Tables 2 and 3.

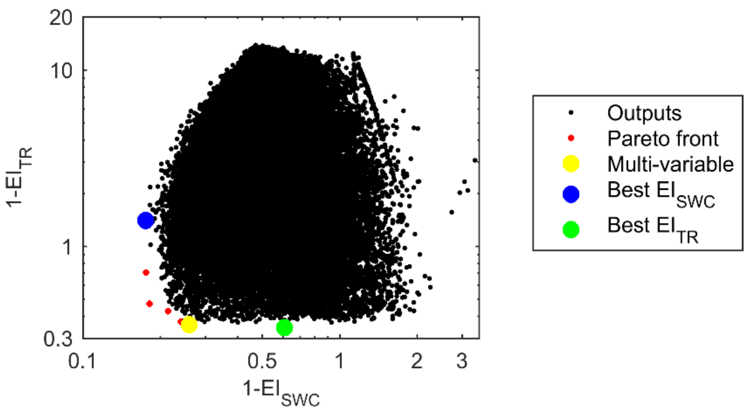

Figure 4 Multi-variable and multi-objective scatterplot for the LEACHM model

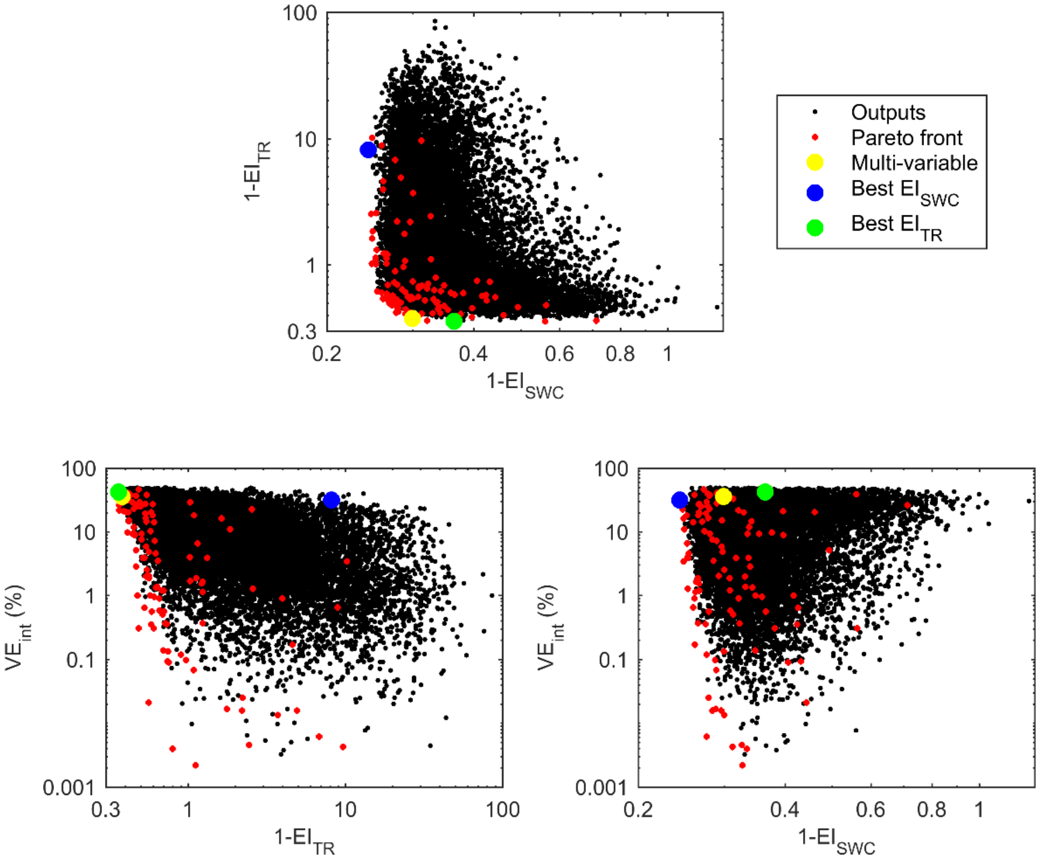

Figure 5 Multi-variable and multi-objective scatterplots for the TETIS model

Parameter	Units	Multi-variable	Best EI_{SWC}	Best EI_{TR}	Range	Reference
Depth to water table	m	47.92	54.10	39.91	20-100	Personal experience
Pan factor	[-]	0.278	0.252	0.251	0.25-1	Hutson (2003)
Vegetation cover factor	[-]	0.416	0.690	0.467	0.4-0.7	Field observation
Roots percentage in layer 1	[-]	0.008	0.009	0.028	0.005-0.2	Baquedano and Castillo (2007); Lidón et al. (1999); Personal experience
Roots percentage in layer 2	[-]	0.190	0.107	0.150	0.01-0.2	Baquedano and Castillo (2007); Lidón et al. (1999); Personal experience
Roots percentage in layer 3	[-]	0.235	0.157	0.239	0.1-0.3	Baquedano and Castillo (2007); Lidón et al. (1999); Personal experience
Roots percentage in layer 4	[-]	0.199	0.283	0.174	0.1-0.3	Baquedano and Castillo (2007); Lidón et al. (1999); Personal experience
Roots percentage in layer 5	[-]	0.180	0.221	0.236	0.1-0.3	Baquedano and Castillo (2007); Lidón et al. (1999); Personal experience
Roots percentage in layer 6	[-]	0.146	0.011	0.065	0.01-0.2	Baquedano and Castillo (2007); Lidón et al. (1999); Personal experience
Roots percentage in layer 7	[-]	0.008	0.14	0.085	0.005-0.2	Baquedano and Castillo (2007); Lidón et al. (1999); Personal experience
a coefficient Campbell's equation (layers 1-2)	kPa	-1.687	-2.763	-1.769	(-3.5)-(-1.5)	Lidón et al. (1999)
b coefficient Campbell's equation (layers 1-2)	[-]	2.153	3.227	3.868	2-5	Lidón et al. (1999); Wöhling et al. (2013)
Saturated hydraulic conductivity (layers 1-2)	mm d^{-1}	83.50	108.10	44.08	30-150	Lidón et al. (1999); Wöhling et al. (2013)
a coefficient Campbell's equation (layers 3-4)	kPa	-2.398	-3.148	-2.214	(-4)-(-2)	Lidón et al. (1999)
b coefficient Campbell's equation (layers 3-4)	[-]	4.024	3.052	7.007	3-8	Lidón et al. (1999); Wöhling et al. (2013)
Saturated hydraulic conductivity (layers 3-4)	mm d^{-1}	30.82	72.02	38.86	30-100	Lidón et al. (1999); Wöhling et al. (2013)
a coefficient Campbell's equation (layers 5-6)	kPa	-2.951	-3.719	-3.723	(-4)-(-2.5)	Lidón et al. (1999)
b coefficient Campbell's equation (layers 5-6)	[-]	5.760	5.105	6.462	5-11	Lidón et al. (1999); Wöhling et al. (2013)
Saturated hydraulic conductivity (layers 5-6)	mm d^{-1}	74.57	99.73	36.53	30-100	Lidón et al. (1999); Wöhling et al. (2013)
a coefficient Campbell's equation (layers 6-22)	kPa	-3.777	-3.480	-3.533	(-4)-(-3)	Lidón et al. (1999)
b coefficient Campbell's equation (layers 6-22)	[-]	13.920	8.941	10.967	8-14	Lidón et al. (1999); Wöhling et al. (2013)
Saturated hydraulic conductivity (layers 6-22)	mm d^{-1}	39.223	36.350	32.953	30-50	Lidón et al. (1999); Wöhling et al. (2013)

Table 2 Parameter values obtained during the calibration process of the LEACHM model. Only the parameters included in the automatic calibration are listed.

Parameter	Units	Multi-variable	Best EI_{SWC}	Best EI_{TR}	Range	Reference
Soil depth	m	0.296	0.310	0.282	0.28-0.32	Field observation
Evaporation depth	m	0.138	0.098	0.132	0.05-0.15	Field observation
Puddle storage	mm	0.074	0.092	0.033	0-0.1	Field observation
Wilting point soil moisture	cm cm^{-1}	0.037	0.032	0.054	0.03-0.07	Caylor et al. (2005); Field observation
Optimal point soil moisture	cm cm^{-1}	0.194	0.193	0.186	0.18-0.2	Caylor et al. (2005); Field observation
Field capacity soil moisture of the layer 1	cm cm^{-1}	0.232	0.227	0.209	0.2-0.24	Caylor et al. (2005); Field observation
Field capacity soil moisture of the layer 2	cm cm^{-1}	0.210	0.206	0.210	0.2-0.22	Caylor et al. (2005); Field observation
Infiltration exponent of the first layer	[-]	1.618	1.094	1.615	0-2	GIMHA (2018)
Infiltration exponent of the second layer	[-]	0.360	0.786	0.671	0-1	GIMHA (2018)
Correction factor for ET_0	[-]	0.701	0.833	0.817	0.65-1	GIMHA (2018)
Vegetation cover factor	[-]	0.419	0.552	0.421	0.4-0.7	Field observation
Maximum leaf water storage	mm	2.528	1.621	1.830	1.5-3.5	Ruiz-Pérez et al. (2016a)
LAI_0	m^2 m^{-2}	2.701	1.728	4.329	1.5-6.5	Li et al. (2019)
Soil moisture deficit nonlinearity parameter	[-]	3.237	2.957	3.073	2.8-3.3	Porporato et al. (2001)
Roots percentage in the first layer	[-]	0.334	0.286	0.241	0.1-0.4	Baquedano and Castillo (2007); Pasquato et al. (2015); Ruiz-Pérez et al. (2016a); Personal experience
Fixed roots percentage in the second layer	[-]	0.241	0.250	0.229	0.2-0.5	Personal experience
Soil moisture threshold	cm cm^{-1}	0.155	0.159	0.150	0.14-0.18	Personal experience
Surface infiltration capacity	mm d^{-1}	infinite	infinite	infinite	-	Field observation
Residence time in the surface storage	days	1	1	1	-	Field observation
Percolation capacity to groundwater storage	mm d^{-1}	infinite	infinite	infinite	-	Field observation
Residence time in gravitational storage	days	infinite	infinite	infinite	-	Field observation

Table 3 Parameters values obtained during the calibration process of the TETIS model.

When the single-variable and single-objective calibration was performed by using the soil water content data (Best EI_{SWC} approach), both models accurately reproduced the observed soil water content. As expected, LEACHM, as a model specifically designed to reproduce water movement in soil, obtained better results. Both models reached EI_{SWC} indices above 0.75 (Table 4), which is considered very good performance (Moriasi et al., 2007). A good agreement between the observed and simulated series was observed (Fig. 6) during both calibration and validation periods. Nevertheless, none was able to reproduce the driest periods during which a significant disagreement between the observed and simulated series was obtained. Transpiration was poorly represented. Negative EI_{SWC} values were obtained (Table 4), which meant that the mean observed value was a better predictor than the simulated one (Moriasi et al., 2007). Transpiration was greatly overestimated (Fig.7) and this overestimation led to a compensation between different fluxes. In the case of TETIS, the simulated transpiration value more than doubled the observed one, which led to an almost null net percolation (Table 5).

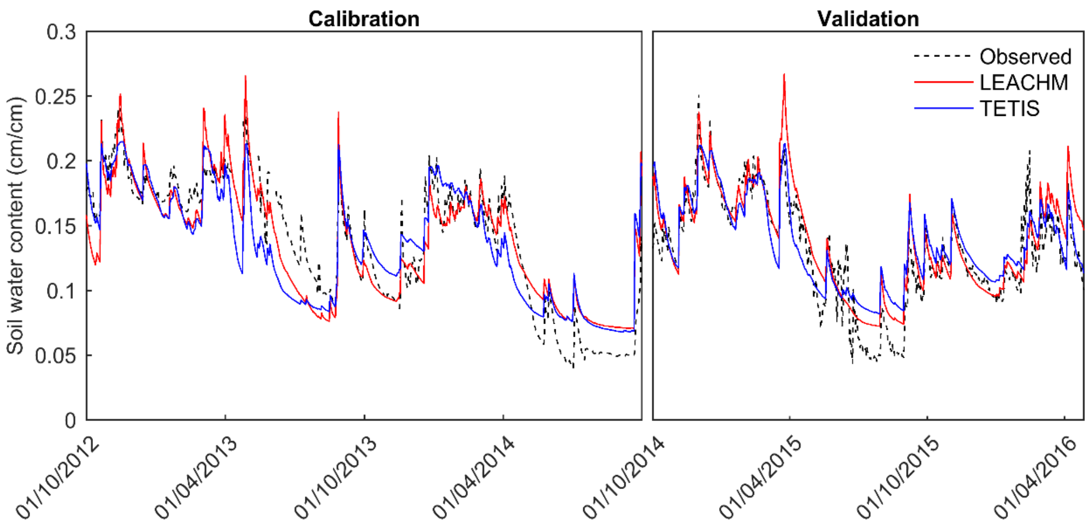

Figure 6 Observed and simulated soil water contents in the single-variable and single-objective calibration by using soil water content

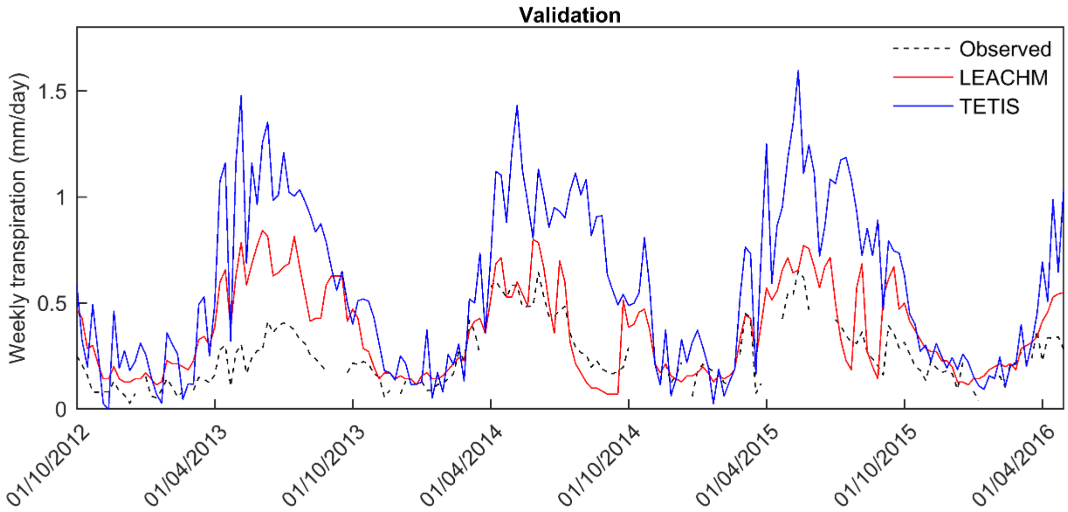

Figure 7 Observed and simulated transpirations in the single-variable and single-objective calibration by using soil water content

Likewise, when the models were calibrated based exclusively on the transpiration data (Best EI_{TR} approach), they acceptably reproduced the transpiration observed values. None reproduced it accurately, but both models presented a satisfactory agreement between the observed and simulated transpiration series (Fig. 8), as well as EI_{TR} indices above 0.5 during the calibration and validation periods (Table 4), which meant satisfactory performance (Moriasi et al., 2007). However, it is worth noting that the performance of both models in reproducing transpiration during the warmest months (June – September), when groundwater transpiration was important, was poor. In contrast to transpiration, soil water content was poorly represented. In LEACHM, soil water content was overestimated (Fig. 9), the EI_{SWC} index dropped down below 0.5 (Table 4) and it led to an unrealistic water balance. The runoff value was 173.2 mm when the observed one was 4.6 mm, and net percolation was negative (Table 5). However, TETIS presented better results. The disagreement reached between the observed and simulated soil water content during the driest months was exacerbated, but a generally satisfactory agreement was shown (Fig. 9) and the EI_{SWC} index was above 0.5 (Table 4).

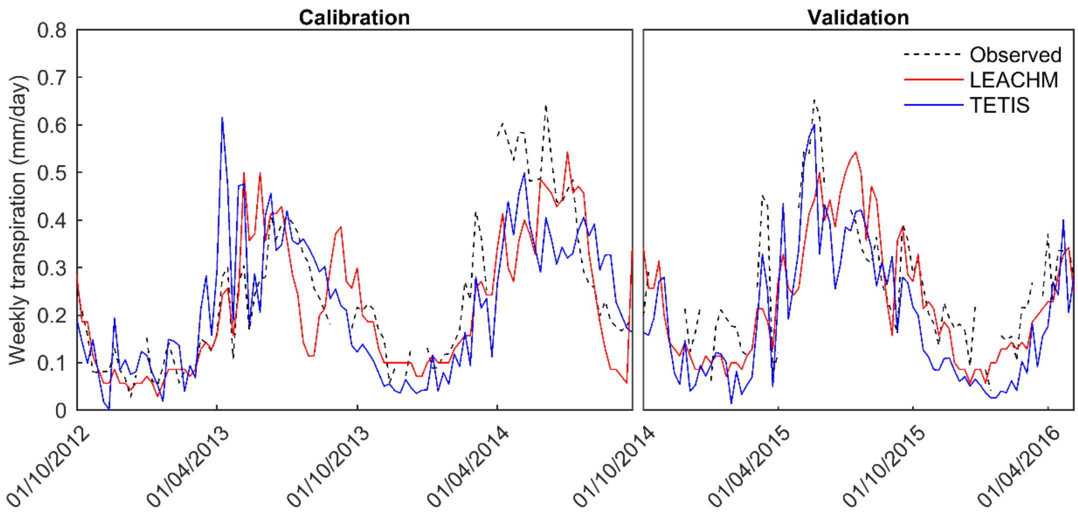

Figure 8 Observed and simulated transpirations in the single-variable and single-objective calibration by using transpiration

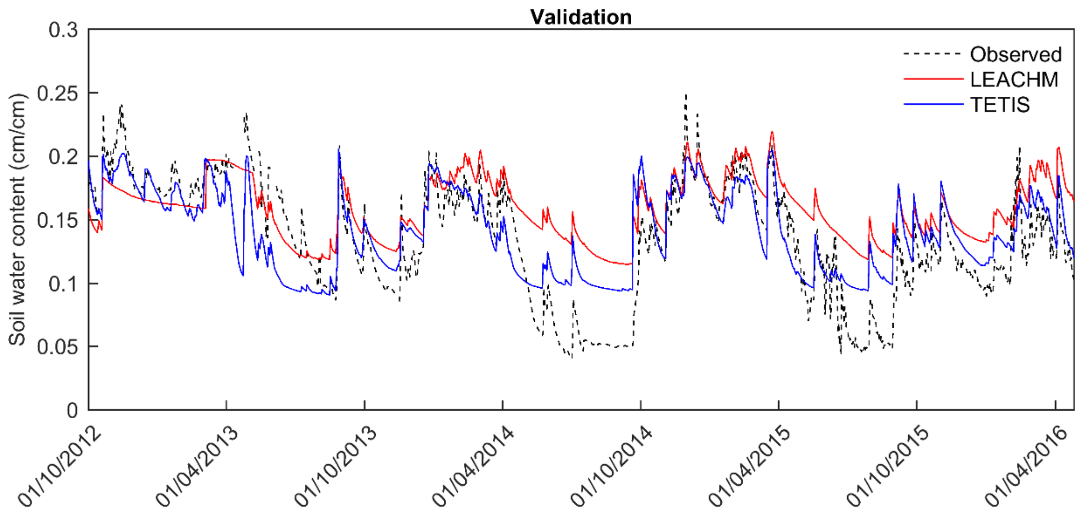

Figure 9 Observed and simulated soil water contents in the single-variable and single-objective calibration by using transpiration

Finally, when the multi-variable and multi-objective calibration was computed (Multi-variable approach), the models' performance to reproduce soil water content or transpiration was generally worse than in the previous calibration approaches (Table 4) when comparing only the calibrated variable results. Moreover, the previous problems were not solved (the lowest soil water content values during the driest periods and transpiration in spring and summer) (Figs. 10 and 11). Nonetheless, both models reproduced the general water dynamics of *Q. ilex* with acceptable accuracy. The soil water content and transpiration data during both the calibration and validation periods were acceptably reproduced (Figs.10 and 11). Realistic values were obtained when the annual balance was calculated, but some differences were found between both models (Table 5).

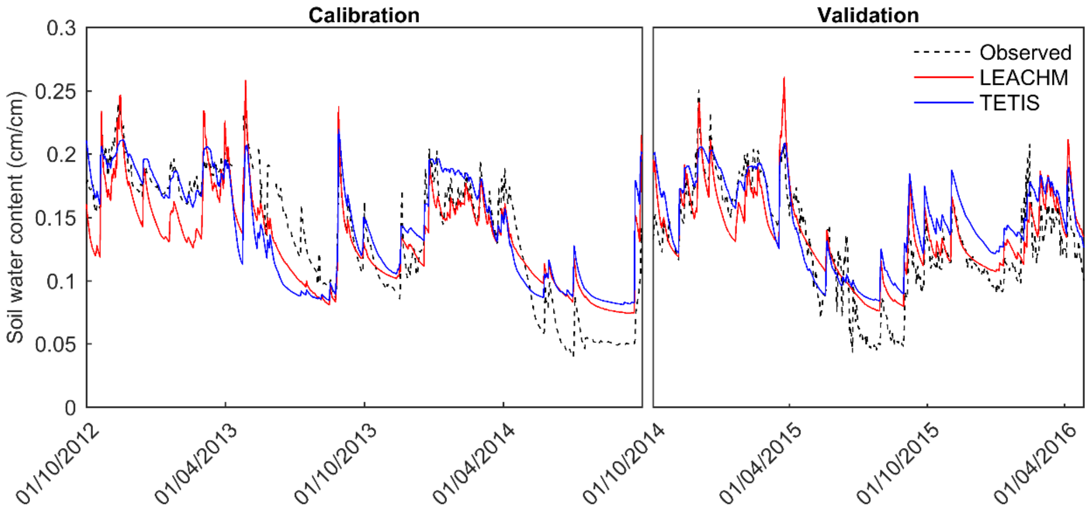

Figure 10 Observed and simulated soil water contents in the multi-variable and multi-objective calibration

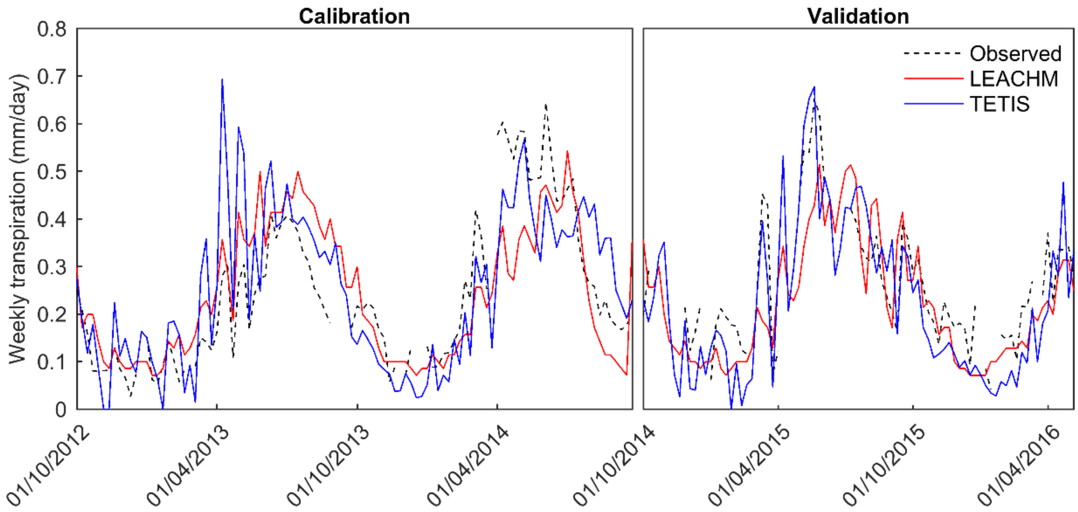

Figure 11 Observed and simulated transpirations in the multi-variable and multi-objective calibration

		Soil water content		Transpiration	
		Calibration	**Validation**	**Calibration**	**Validation**
LEACHM	**Best** EI_{SWC}	0.825	0.773	-	-0.218
	Best EI_{TR}	-	0.286	0.655	0.616
	Multi-variable	0.741	0.737	0.641	0.625
TETIS	**Best** EI_{SWC}	0.757	0.764	-	-6.735
	Best EI_{TR}	-	0.636	0.639	0.624
	Multi-variable	0.700	0.595	0.619	0.721

Table 4 E indices obtained in each calibration approach

Flows (mm)	Obs.	LEACHM model			TETIS model		
		Multi-variable	Best EI_{SWC}	Best EI_{TR}	Multi-variable	Best EI_{SWC}	Best EI_{TR}
Precipitation	426.2	-	-	-	426.2	426.2	426.2
Interception	129.2	-	-	-	81.4	86.7	72.9
Net precipitation	297.1	297.1	297.1	297.1	344.8	339.6	353.4
Soil evaporation	-	64.4	48.2	44.9	118.7	114.7	123.2
Soil transpiration	-	68.9	101.0	55.1	49.6	70.5	42.1
Groundwater transpiration	-	21.0	37.3	29.9	44.2	156.6	40.1
Total transpiration	101.6	89.9	138.3	85.0	93.7	227.1	82.2
Runoff	4.6	3.0	0.0	173.2	0.0	0.0	0.0
Percolation	-	161.8	151.1	26.4	181.6	160.2	193.0
Net percolation	-	140.8	113.9	-3.5	137.5	3.6	152.9

Table 5 Mean annual water balances (2012-2015)

The main difference remained in evapotranspiration partitioning. Despite including interception in the calibration process, TETIS underestimated it, which led to higher soil evaporation. Although both models obtained similar total transpiration values, the soil transpiration in LEACHM was higher than that calculated by TETIS. In any case, these ecosystems showed a strong dependence on groundwater. The relative contributions of groundwater transpiration to total transpiration, summer transpiration and evapotranspiration were calculated (Table 6). TETIS showed a stronger dependence for *Q.ilex* on groundwater resources.

	Transpiration	Transpiration (summer months)	Evapotranspiration
LEACHM	23.4%	42.3%	7.4%
TETIS	47.2%	76.4%	15.0%

Table 6 Relative contributions of groundwater transpiration to total transpiration, summer transpiration and total evapotranspiration

The annual balances of each hydrological year and their B/G rates were calculated. These results also showed that *Q.ilex* depended on increased groundwater resources when precipitation reduced (Table 7). Both models obtained low soil transpiration values and high groundwater transpiration in the driest year (2013-2014), while dependence was weaker in the wettest year (2012-2013). Both models obtained B/G rates below 1.

This value was around 0.1 in the driest year, and bigger differences were obtained in the wettest year (Table 8). LEACHM and TETIS respectively obtained a value of around 0.6 and 0.8.

Flows (mm)	LEACHM model			TETIS model		
	12-13	13-14	14-15	12-13	13-14	14-15
Precipitation	-	-	-	581.2	271.1	426.4
Interception	-	-	-	105.4	63.0	75.9
Net precipitation	395.1	190.8	305.3	475.9	208.1	350.5
Soil evaporation	80.1	53.8	59.3	135.6	87.9	132.7
Soil transpiration	75.1	59.4	72.1	62.1	36.1	50.5
Groundwater transpiration	18.5	23.6	20.9	29.8	53.7	48.9
Total transpiration	93.6	83.0	93.0	92.0	89.8	99.4
Runoff	7.6	0.0	1.3	0.0	0.0	0.0
Percolation	241.5	57.8	186.2	297.4	69.4	178.1
Net percolation	223.0	34.2	165.3	267.5	15.7	129.2
Storage variation	-10.8	+19.5	-14.7	-19.3	+14.7	-10.8

Table 7 Annual water balances obtained from the multi-variable and multi-objective calibration for the three complete hydrological years

	LEACHM model			TETIS model			del Campo et al. (2019a)		
	12-13	13-14	14-15	12-13	13-14	14-15	12-13	13-14	14-15
Green water (mm)	359.8	217.1	273.4	333.0	240.7	308.0	312.6	211.0	254.9
Blue water (mm)	230.6	34.2	166.6	267.5	15.7	129.2	268.6	60.1	171.6
B/G ratio	0.64	0.16	0.61	0.80	0.07	0.42	0.86	0.28	0.67

Table 8 The Blue (runoff+percolation) and Green (evapotranspiration) rates of each model

4 Discussion

Both the single-variable and single-objective calibration approaches indicated problems in reproducing the state variable not included in the calibration process, and led to unrealistic annual balances. As previously mentioned, a single-variable and single-objective calibration is usually inadequate for measuring all system's characteristics (Guo et al., 2013; Yapo et al., 1998), a problem that was evidenced in this case. Both models reproduced the calibrated variable with a high degree of accuracy, but were unable to represent the other state variable and fluxes compensated one another, which led to unrealistic hydrological balance representations (Li et al., 2018; Rankinen et al., 2006). When the models were calibrated with only the soil water content data, the parameters were optimised to obtain the best soil water content representation, and transpiration in both models increased. LEACHM obtained high values for vegetation cover fraction and hydraulic conductivities, and TETIS obtained high vegetation cover fraction values, but low field capacity soil moisture values. These parameter values allowed the models to properly reproduce fast soil water content changes because transpiration increased, but they were not optimum to represent the whole system. Likewise when they were calibrated by using transpiration, LEACHM obtained lower vegetation cover factor and hydraulic conductivity values, while TETIS also obtained lower vegetation cover factor and field capacity soil moisture values. Consequently, transpiration was reduced to fit the observed values, but soil water content and hydrological balance were poorly represented.

Conversely, the multi-variable and multi-objective calibration obtained a compromise solution between both single-variable and single-objective calibrations. The two models acceptably reproduced the water dynamics of *Q.ilex*. Soil water content was reproduced more accurately than transpiration, despite the disagreement between the observed and simulated soil water contents in the driest months. Nonetheless, this disagreement and their poor performance in reproducing transpiration can be explained by both models' simple transpiration representation. LEACHM uses weekly averaged potential evapotranspiration values, but its time step is not weekly and it does not consider interception, which leads to a very low pan factor value to compensate the energy used during intercepted water evaporation. TETIS divides soil into only two layers and, although the introduction of parameter LAI_0 improved its performance, it can be oversimplified.

Regarding the hydrological balance obtained with the multi-variable and multi-objective calibration, the results of both models showed how *Q. ilex* strongly depends on groundwater resources. Hence given the climate change projections in the Mediterranean region (Spinoni et al., 2018), proper transpiration quantification, as well as correct distribution between the water that flows out of the ecosystem and evapotranspiration, are crucial to face problems related to water resource assessments, forest management or agriculture (Reyes-Acosta and Lubczynski, 2013; Tie et al., 2018).

In this case, both models were able to reproduce the observed total transpiration, but differences were found in evapotranspiration partitioning. Firstly, TETIS underestimated the interception and this error was compensated by an increment in soil evaporation. LEACHM, which does not consider interception, obtained an average soil evaporation value of 64.4 mm, which comes very close to the value reported by del Campo et al. (2019a) in this same plot, which was 47 mm (43-51 mm). The value obtained by TETIS was 118.7 mm, but the error in interception was 47.8 mm, which is almost the difference between the soil evaporation simulated by LEACHM and that simulated by TETIS. Secondly, different soil and groundwater transpiration values were obtained. The average contribution of groundwater transpiration to total transpiration was 23.4% and 47.2%, while the contribution to total evapotranspiration was 7.4% and 15%, both respectively in LEACHM and TETIS. These differences seem high, but these values fall within the ranges indicated in previous studies. Hubbert et al. (2001) found that the contribution of weathered bedrock to total transpiration was 70% in a *Pinus jeffreyi* plantation in a Mediterranean climate. Hassan et al. (2014) reported that the groundwater contribution to total evapotranspiration was 6.7% in a mixed *Q. ilex* and *Q. pyrenaica* open forest in a semiarid climate. Nonetheless, it should be highlighted that the tree density at our study site was higher than that indicated in Hassan et al. (2014), thus this value may be higher. Moreover, if the contribution of groundwater transpiration to total transpiration is computed in summer months when dependence increased, these values were 42.3% and 76.4% in LEACHM and TETIS, respectively, and were similar to the results obtained in previous studies. David et al. (2007) found that groundwater transpiration was 70% of total transpiration in summer months in a *Q. ilex* and *Q. suber* woodland in a semiarid climate, and in the above-mentioned *Q. ilex* and *Q. pyrenaica* woodland, Balugani et al. (2017) reported that groundwater transpiration was 50% of total transpiration. In addition, both models showed similar dynamics. The dependence of *Q.ilex* on groundwater resources increased in the driest year in both models, which coincides with Eliades et al. (2018) in a *Pinus brutia* forest in a Mediterranean climate, where groundwater transpiration increased from 65.6% to 77% of total transpiration.

Finally, no conspicuous differences were found in the B/G rates estimations. Both models obtained rates below 1, which indicates that less than half the precipitation supplies the system. These values were compared to those obtained with the data of del Campo et al. (2019a) and they were alike. However, LEACHM obtained more similar rates than TETIS did. In TETIS, the difference between both rates for the driest year was significant.

5 Conclusions

In this study, a multi-variable calibration with a multi-objective approach was carried out to explain the hydrological behaviour of facultative phreatophytes under semiarid conditions using two models with different conceptualisations. This multi-variable and multi-objective calibration was compared to the traditional single-variable and single-objective calibration approach. Our results suggest that a multi-variable and multi-objective calibration, provided enough data are available, is a necessary tool to reproduce the water dynamics of a facultative phreatophytic forest keeping the parameter sets as realistic as possible. In contrast, the single-variable and single-objective calibration was able to reproduce the calibrated state variable (soil moisture or transpiration) with a high degree of accuracy, but poorly represented other state variables of the system or led to an unreal water balance closure. Moreover, the similarity of the results obtained by both models, despite their different conceptualisations, reinforces the robustness of using multi-variable and multi-objective calibration.

The multi-variable and multi-objective calibration results showed how *Q. ilex* strongly depends on groundwater resources. In semiarid environments with shallow soils, water transpiration from groundwater is an important water source for these forests, especially in dry years. This dependence in the driest year in our case study increased and, in summer months due to fast soil water depletion, this contribution reached crucial values. Consequently, during prolonged drought periods, such forests will suffer severe effects. Therefore, it is clear that hydrological models applied in semiarid regions should include the groundwater transpiration mechanism because such forests can heavily influence future water availability. In this sense, both LEACHM and TETIS mechanisms to reproduce groundwater transpiration proved an acceptable tool to be applied in the regions covered by these phreatophytic species. However, it is worth noting that LEACHM has high parameter requirements compared to TETIS.

Conflict of interest

The authors have no conflict of interest to declare.

Acknowledgements

This work was supported by the Spanish Ministry of Science and Innovation through the research projects: TETISMED (CGL2014-58127-C3-3-R), SILWAMED (CGL2014-58127-C3-2-R) and TETISCHANGE, and by the project LIFE17 CCA/ES/000063 RESILIENTFORESTS. The anonymous reviewers whose comments improved the quality of the paper.

References

Abbaspour, K.C., Yang, J., Maximov, I., Siber, R., Bogner, K., Mieleitner, J., Zobrist, J., Srinivasan, R., 2007. Modelling hydrology and water quality in the pre-alpine/alpine Thur watershed using SWAT. J. Hydrol. 333, 413–430. https://doi.org/10.1016/J.JHYDROL.2006.09.014

Asada, K., Eguchi, S., Urakawa, R., Itahashi, S., Matsumaru, T., Nagasawa, T., Aoki, K., Nakamura, K., Katou, H., 2013. Modifying the LEACHM model for process-based prediction of nitrate leaching from cropped Andosols. Plant Soil 373, 609–625. https://doi.org/10.1007/s11104-013-1809-7

Balugani, E., Lubczynski, M.W., Reyes-Acosta, L., van der Tol, C., Francés, A.P., Metselaar, K., 2017. Groundwater and unsaturated zone evaporation and transpiration in a semi-arid open woodland. J. Hydrol. 547, 54–66. https://doi.org/10.1016/j.jhydrol.2017.01.042

Baquedano, F.J., Castillo, F.J., 2007. Drought tolerance in the Mediterranean species Quercus coccifera, Quercus ilex, Pinus halepensis, and Juniperus phoenicea. Photosynthetica 45, 229–238. https://doi.org/10.1007/s11099-007-0037-x

Barbeta, A., Peñuelas, J., 2017. Relative contribution of groundwater to plant transpiration estimated with stable isotopes. Sci. Rep. 7, 10580. https://doi.org/10.1038/s41598-017-09643-x

Barbeta, A., Peñuelas, J., 2016. Sequence of plant responses to droughts of different timescales: lessons from holm oak (Quercus ilex) forests. Plant Ecol. Divers. 9, 321–338. https://doi.org/10.1080/17550874.2016.1212288

Bautista, I., Pabón, C., Lull, C., González-Sanchís, M., Lidón, A., Del Campo, A.D., 2015. Efectos de la gestión forestal en los flujos de nutrientes asociados al ciclo hidrológico en un bosque mediterráneo de Quercus Ilex. Cuad. la Soc. Española Ciencias For. 41, 343–354.

Beven, K., 1993. Prophecy, reality and uncertainty in distributed hydrological modelling. Adv. Water Resour. 16, 41–51. https://doi.org/10.1016/0309-1708(93)90028-E

Burgess, S.S.O., Adams, M.A., Turner, N.C., Beverly, C.R., Ong, C.K., Khan, A.A., Bleby, T.M., 2001. An improved heat pulse method to measure low and reverse rates of sap flow in woody plants. Tree Physiol. 21, 589–98.

Campbell, G.S., 1974. A simple method for determining unsaturated conductivity from moisture retention data. Soil Sci. 117, 311–314. https://doi.org/10.1097/00010694-197406000-00001

Canadell, J., Jackson, R.B., Ehleringer, J.R., Mooney, H.A., Sala, O.E., Schulze, E.D., 1996. Maximum rooting depth of vegetation types at the global scale. Oecologia 108, 583–595. https://doi.org/10.1007/BF00329030

Cao, W., Bowden, W.B., Davie, T., Fenemor, A., 2006. Multi-variable and multi-site calibration and validation of SWAT in a large mountainous catchment with high spatial variability. Hydrol. Process. 20, 1057–1073. https://doi.org/10.1002/hyp.5933

Caylor, K.K., Manfreda, S., Rodriguez-Iturbe, I., 2005. On the coupled geomorphological and ecohydrological organization of river basins. Adv. Water Resour. 28, 69–86. https://doi.org/10.1016/j.advwatres.2004.08.013

Cook, B.I., Mankin, J.S., Anchukaitis, K.J., 2018. Climate Change and Drought: From Past to Future. Curr. Clim. Chang. Reports 4, 164–179. https://doi.org/10.1007/s40641-018-0093-2

Crank, J., Nicolson, P., 1947. A practical method for numerical evaluation of solutions of partial differential equations of the heat-conduction type. Math. Proc. Cambridge Philos. Soc. 43, 50–67. https://doi.org/10.1017/S0305004100023197

David, T.S., Ferreira, M.I., Cohen, S., Pereira, J.S., David, J.S., 2004. Constraints on transpiration from an evergreen oak tree in southern Portugal. Agric. For. Meteorol. 122, 193–205. https://doi.org/10.1016/j.agrformet.2003.09.014

David, T.S., Henriques, M.O., Kurz-Besson, C., Nunes, J., Valente, F., Vaz, M., Pereira, J.S., Siegwolf, R., Chaves, M.M., Gazarini, L.C., David, J.S., 2007. Water-use strategies in two co-occurring Mediterranean evergreen oaks: Surviving the summer drought. Tree Physiol. 27, 793–803. https://doi.org/10.1093/treephys/27.6.793

del Campo, A.D., González-Sanchis, M., García-Prats, A., Ceacero, C.J., Lull, C., 2019a.

The impact of adaptive forest management on water fluxes and growth dynamics in a water-limited low-biomass oak coppice. Agric. For. Meteorol. 264, 266–282. https://doi.org/10.1016/j.agrformet.2018.10.016

del Campo, A.D., González-Sanchis, M., Lidón, A., Ceacero, C.J., García-Prats, A., 2018. Rainfall partitioning after thinning in two low-biomass semiarid forests: Impact of meteorological variables and forest structure on the effectiveness of water-oriented treatments. J. Hydrol. 565, 74–86. https://doi.org/10.1016/J.JHYDROL.2018.08.013

del Campo, A.D., González-Sanchis, M., Molina, A.J., García-Prats, A., Ceacero, C.J., Bautista, I., 2019b. Effectiveness of water-oriented thinning in two semiarid forests: The redistribution of increased net rainfall into soil water, drainage and runoff. For. Ecol. Manage. 438, 163–175. https://doi.org/10.1016/J.FORECO.2019.02.020

Deng, Z., Guan, H., Hutson, J., Forster, M.A., Wang, Y., Simmons, C.T., 2017. A vegetation-focused soil-plant-atmospheric continuum model to study hydrodynamic soil-plant water relations. Water Resour. Res. 53, 4965–4983. https://doi.org/10.1002/2017WR020467

Eliades, M., Bruggeman, A., Lubczynski, M.W., Christou, A., Camera, C., Djuma, H., 2018. The water balance components of Mediterranean pine trees on a steep mountain slope during two hydrologically contrasting years. J. Hydrol. 562, 712–724. https://doi.org/10.1016/j.jhydrol.2018.05.048

Fan, Y., Li, H., Miguez-Macho, G., 2013. Global patterns of groundwater table depth. Science (80-.). 339, 940–943. https://doi.org/10.1126/science.1229881

Francés, F., Vélez, J.I., Vélez, J.J., 2007. Split-parameter structure for the automatic calibration of distributed hydrological models. J. Hydrol. 332, 226–240. https://doi.org/10.1016/J.JHYDROL.2006.06.032

Gallart, F., Llorens, P., Latron, J., Regüés, D., 2002. Hydrological processes and their seasonal controls in a small Mediterranean mountain catchment in the Pyrenees. Hydrol. Earth Syst. Sci. 6, 527–537. https://doi.org/10.5194/hess-6-527-2002

García-Ruiz, J.M., López-Moreno, I.I., Vicente-Serrano, S.M., Lasanta-Martínez, T., Beguería, S., 2011. Mediterranean water resources in a global change scenario. Earth-Science Rev. https://doi.org/10.1016/j.earscirev.2011.01.006

GIMHA, 2018. Description of the Distributed Conceptual Hydrological Model Tetis V.9.0.1. Research Group of Hydrological and Environmental Modelling, Universitat Politècnica de València, Valencia, Spain.

Granier, A., Loustau, D., Bréda, N., 2000. A generic model of forest canopy conductance dependent on climate, soil water availability and leaf area index. Ann. For. Sci. 57, 755–765. https://doi.org/10.1051/forest:2000158

Guo, J., Zhou, J., Lu, J., Zou, Q., Zhang, H., Bi, S., 2014. Multi-objective optimization of empirical hydrological model for streamflow prediction. J. Hydrol. 511, 242–253. https://doi.org/10.1016/j.jhydrol.2014.01.047

Guo, J., Zhou, J., Zou, Q., Liu, Y., Song, L., 2013. A Novel Multi-Objective Shuffled Complex Differential Evolution Algorithm with Application to Hydrological Model Parameter Optimization. Water Resour. Manag. 27, 2923–2946. https://doi.org/10.1007/s11269-013-0324-1

Haas, M.B., Guse, B., Pfannerstill, M., Fohrer, N., 2016. A joined multi-metric calibration of river discharge and nitrate loads with different performance measures. J. Hydrol. 536, 534–545. https://doi.org/10.1016/j.jhydrol.2016.03.001

Hargreaves, G.H., Samani, Z.A., 1985. Reference Crop Evapotranspiration from Temperature. Appl. Eng. Agric. 1, 96–99. https://doi.org/10.13031/2013.26773

Hasan, M.A., Pradhanang, S.M., 2017. Estimation of flow regime for a spatially varied

Himalayan watershed using improved multi-site calibration of the Soil and Water Assessment Tool (SWAT) model. Environ. Earth Sci. 76, 787. https://doi.org/10.1007/s12665-017-7134-3

Hassan, S.M.M.T., Lubczynski, M.W., Niswonger, R.G., Su, Z., 2014. Surface-groundwater interactions in hard rocks in Sardon Catchment of western Spain: An integrated modeling approach. J. Hydrol. 517, 390–410. https://doi.org/10.1016/j.jhydrol.2014.05.026

Her, Y., Chaubey, I., 2015. Impact of the numbers of observations and calibration parameters on equifinality, model performance, and output and parameter uncertainty. Hydrol. Process. 29, 4220–4237. https://doi.org/10.1002/hyp.10487

Herman, M.R., Nejadhashemi, A.P., Abouali, M., Hernandez-Suarez, J.S., Daneshvar, F., Zhang, Z., Anderson, M.C., Sadeghi, A.M., Hain, C.R., Sharifi, A., 2018. Evaluating the role of evapotranspiration remote sensing data in improving hydrological modeling predictability. J. Hydrol. 556, 39–49. https://doi.org/10.1016/j.jhydrol.2017.11.009

Hubbert, K.R., Graham, R.C., Anderson, M.A., 2001. Soil and weathered bedrock: Components of a Jeffrey pine plantation substrate. Soil Sci. Soc. Am. J. 65, 1255–1262. https://doi.org/10.2136/sssaj2001.6541255x

Hutson, J.L., 2003. LEACHM - Leaching Estimation and Chemistry Model. Department of Crop and Soil Sciences, Cornell University, Ithaca, New York, Ithaca, New York.

Khu, S.T., Madsen, H., 2005. Multiobjective calibration with Pareto preference ordering: An application to rainfall-runoff model calibration. Water Resour. Res. 41, 1–14. https://doi.org/10.1029/2004WR003041

Li, X., Gentine, P., Lin, C., Zhou, S., Sun, Z., Zheng, Y., Liu, J., Zheng, C., 2019. A simple and objective method to partition evapotranspiration into transpiration and evaporation at eddy-covariance sites. Agric. For. Meteorol. 265, 171–182. https://doi.org/10.1016/j.agrformet.2018.11.017

Li, Y., Grimaldi, S., Pauwels, V.R.N., Walker, J.P., 2018. Hydrologic model calibration using remotely sensed soil moisture and discharge measurements: The impact on predictions at gauged and ungauged locations. J. Hydrol. 557, 897–909. https://doi.org/10.1016/j.jhydrol.2018.01.013

Lidón, A., Ramos, C., Ginestar, D., Contreras, W., 2013. Assessment of LEACHN and a simple compartmental model to simulate nitrogen dynamics in citrus orchards. Agric. Water Manag. 121, 42–53. https://doi.org/10.1016/j.agwat.2013.01.008

Lidón, A., Ramos, C., Rodrigo, A., 1999. Comparison of drainage estimation methods in irrigated citrus orchards. Irrig. Sci. 19, 25–36. https://doi.org/10.1007/s002710050068

López López, P., Wanders, N., Schellekens, J., Renzullo, L.J., Sutanudjaja, E.H., Bierkens, M.F.P., 2016. Improved large-scale hydrological modelling through the assimilation of streamflow and downscaled satellite soil moisture observations. Hydrol. Earth Syst. Sci. 20, 3059–3076. https://doi.org/10.5194/hess-20-3059-2016

Lubczynski, M.W., 2009. The hydrogeological role of trees in water-limited environments. Hydrogeol. J. 17, 247–259. https://doi.org/10.1007/s10040-008-0357-3

Macfarlane, C., Grigg, A., McGregor, R., Ogden, G., Silberstein, R., 2018. Overstorey evapotranspiration in a seasonally dry Mediterranean eucalypt forest: Response to groundwater and mining. Ecohydrology 11, 17. https://doi.org/10.1002/eco.1971

Medici, C., Wade, A.J., Francés, F., 2012. Does increased hydrochemical model complexity decrease robustness? J. Hydrol. 440–441, 1–13. https://doi.org/10.1016/j.jhydrol.2012.02.047

Mertens, J., Madsen, H., Kristensen, M., Jacques, D., Feyen, J., 2005. Sensitivity of soil parameters in unsaturated zone modelling and the relation between effective, laboratory and in situ estimates. Hydrol. Process. 19, 1611–1633. https://doi.org/10.1002/hyp.5591

Miller, G.R., Chen, X., Rubin, Y., Ma, S., Baldocchi, D.D., 2010. Groundwater uptake by woody vegetation in a semiarid oak savanna. Water Resour. Res. 46. https://doi.org/10.1029/2009WR008902

Moriasi, D.N., Arnold, J.G., Van Liew, M.W., Bingner, R.L., Harmel, R.D., Veith, T.L., 2007. Model Evaluation Guidelines for Systematic Quantification of Accuracy in Watershed Simulations. Trans. ASABE 50, 885–900. https://doi.org/10.13031/2013.23153

Morillas, L., Leuning, R., Villagarcía, L., García, M., Serrano-Ortiz, P., Domingo, F., 2013. Improving evapotranspiration estimates in Mediterranean drylands: The role of soil evaporation. Water Resour. Res. 49, 6572–6586. https://doi.org/10.1002/wrcr.20468

Nasri, N., Chebil, M., Guellouz, L., Bouhlila, R., Maslouhi, A., Ibnoussina, M., 2015. Modelling nonpoint source pollution by nitrate of soil in the Mateur plain, northeast of Tunisia. Arab. J. Geosci. 8, 1057–1075. https://doi.org/10.1007/s12517-013-1215-8

Nimah, M.N., Hanks, R.J., 1973. Model for Estimating Soil Water, Plant, and Atmospheric Interrelations: I. Description and Sensitivity. Soil Sci. Soc. Am. J. 37, 522–527. https://doi.org/10.2136/sssaj1973.03615995003700040018x

Nkiaka, E., Nawaz, N.R., Lovett, J.C., 2018. Effect of single and multi-site calibration techniques on hydrological model performance, parameter estimation and predictive uncertainty: a case study in the Logone catchment, Lake Chad basin. Stoch. Environ. Res. Risk Assess. 32, 1665–1682. https://doi.org/10.1007/s00477-017-1466-0

Pasquato, M., Medici, C., Friend, A.D., Francés, F., 2015. Comparing two approaches for parsimonious vegetation modelling in semiarid regions using satellite data. Ecohydrology 8, 1024–1036. https://doi.org/10.1002/eco.1559

Piñol, J., Lledó, M.J., Escarré, A., 1991. Hydrological balance of two Mediterranean forested catchments (Prades, northeast Spain). Hydrol. Sci. J. 36, 95–107. https://doi.org/10.1080/02626669109492492

Porporato, A., Laio, F., Ridolfi, L., Rodriguez-Iturbe, I., 2001. Plants in water-controlled ecosystems: active role in hydrologic processes and response to water stress III. Vegetation water stress. Adv. Water Resour. 24, 725–744. https://doi.org/10.1016/S0309-1708(01)00006-9

Rankinen, K., Karvonen, T., Butterfield, D., 2006. An application of the GLUE methodology for estimating the parameters of the INCA-N model. Sci. Total Environ. 365, 123–139. https://doi.org/10.1016/J.SCITOTENV.2006.02.034

Reyes-Acosta, J.L., Lubczynski, M.W., 2013. Mapping dry-season tree transpiration of an oak woodland at the catchment scale, using object-attributes derived from satellite imagery and sap flow measurements. Agric. For. Meteorol. 174–175, 184–201. https://doi.org/10.1016/j.agrformet.2013.02.012

Rientjes, T.H.M., Muthuwatta, L.P., Bos, M.G., Booij, M.J., Bhatti, H.A., 2013. Multi-variable calibration of a semi-distributed hydrological model using streamflow data and satellite-based evapotranspiration. J. Hydrol. 505, 276–290. https://doi.org/10.1016/j.jhydrol.2013.10.006

Rodriguez-Iturbe, I., Porporato, A., Laio, F., Ridolfi, L., 2001. Plants in water-controlled ecosystems: active role in hydrologic processes and response to water stress I. Scope and general outline. Adv. Water Resour. 24, 695–705. https://doi.org/10.1016/S0309-1708(01)00004-5

Ruiz-Pérez, G., González-Sanchis, M., Del Campo, A.D., Francés, F., 2016a. Can a parsimonious model implemented with satellite data be used for modelling the vegetation dynamics and water cycle in water-controlled environments? Ecol. Modell. 324, 45–53. https://doi.org/10.1016/j.ecolmodel.2016.01.002

Ruiz-Pérez, G., Medici, C., Latron, J., Llorens, P., Gallart, F., Francés, F., 2016b. Investigating the behaviour of a small Mediterranean catchment using three different hydrological models as hypotheses. Hydrol. Process. 30, 2050–2062. https://doi.org/10.1002/hyp.10738

Schwinning, S., 2010. The ecohydrology of roots in rocks. Ecohydrology 3, 238–245. https://doi.org/10.1002/eco.134

Spinoni, J., Vogt, J. V., Naumann, G., Barbosa, P., Dosio, A., 2018. Will drought events become more frequent and severe in Europe? Int. J. Climatol. 38, 1718–1736. https://doi.org/10.1002/joc.5291

Swaffer, B.A., Holland, K.L., Doody, T.M., Li, C., Hutson, J., 2014. Water use strategies of two co-occurring tree species in a semi-arid karst environment. Hydrol. Process. 28, 2003–2017. https://doi.org/10.1002/hyp.9739

Tie, Q., Hu, H., Tian, F., Holbrook, N.M., 2018. Comparing different methods for determining forest evapotranspiration and its components at multiple temporal scales. Sci. Total Environ. 633, 12–29. https://doi.org/10.1016/j.scitotenv.2018.03.082

Vicente, E., Vilagrosa, A., Ruiz-Yanetti, S., Manrique-Alba, À., González-Sanchís, M., Moutahir, H., Chirino, E., del Campo, A., Bellot, J., 2018. Water balance of Mediterranean Quercus ilex L. and Pinus halepensis mill. forests in semiarid climates: A review in a climate change context. Forests. https://doi.org/10.3390/f9070426

Vrugt, J.A., Gupta, H. V., Bastidas, L.A., Bouten, W., Sorooshian, S., 2003. Effective and efficient algorithm for multiobjective optimization of hydrologic models. Water Resour. Res. 39. https://doi.org/10.1029/2002WR001746

Williams, J.R., 1991. Runoff and Water Erosion, in: Modeling Plant and Soil Systems. American Society of Agronomy, Crop Science Society of America, Soil Science Society of America, Madison, WI 53711, USA, pp. 439–455. https://doi.org/10.2134/agronmonogr31.c18

Witty, J.H., Graham, R.C., Hubbert, K.R., Doolittle, J.A., Wald, J.A., 2003. Contributions of water supply from the weathered bedrock zone to forest soil quality. Geoderma 114, 389–400. https://doi.org/10.1016/S0016-7061(03)00051-X

Wöhling, T., Gayler, S., Priesack, E., Ingwersen, J., Wizemann, H.D., Högy, P., Cuntz, M., Attinger, S., Wulfmeyer, V., Streck, T., 2013. Multiresponse, multiobjective calibration as a diagnostic tool to compare accuracy and structural limitations of five coupled soil-plant models and CLM3.5. Water Resour. Res. 49, 8200–8221. https://doi.org/10.1002/2013WR014536

Yapo, P.O., Gupta, H.V., Sorooshian, S., 1998. Multi-objective global optimization for hydrologic models. J. Hydrol. 204, 83–97. https://doi.org/10.1016/S0022-1694(97)00107-8

Yaseef, N.R., Yakir, D., Rotenberg, E., Schiller, G., Cohen, S., 2010. Ecohydrology of a semi-arid forest: Partitioning among water balance components and its implications for predicted precipitation changes. Ecohydrology 3, 143–154. https://doi.org/10.1002/eco.65

Zhang, J., Li, Q., Guo, B., Gong, H., 2015. The comparative study of multi-site uncertainty evaluation method based on SWAT model. Hydrol. Process. 29, 2994–3009. https://doi.org/10.1002/hyp.10380

Zhang, Y., Peña-Arancibia, J.L., McVicar, T.R., Chiew, F.H.S., Vaze, J., Liu, C., Lu, X., Zheng, H., Wang, Y., Liu, Y.Y., Miralles, D.G., Pan, M., 2016. Multi-decadal trends in global terrestrial evapotranspiration and its components. Sci. Rep. 6, 1–12. https://doi.org/10.1038/srep19124